UNIVERSITY OF STRATHCLYDE
DEPARTMENT OF MATHEMATICS

Computational Fluid Dynamics for Nematic Liquid Crystals

by

André M. Sonnet and Alison Ramage

Strathclyde Mathematics Research Report No. 28 (2007)
November 2007

Computational Fluid Dynamics for Nematic Liquid Crystals

André M. Sonnet* Alison Ramage†

November 6, 2007

Abstract

We consider a nematic liquid crystal in a spatially inhomogeneous flow situation. The orientational order is described by a second rank alignment tensor because of the defects that inevitably occur. The evolution is determined by two equations. The flow is governed by a generalised Stokes equation in which the divergence of the stress tensor also depends on the alignment tensor and its time derivative. The evolution of the alignment is governed by a convection-diffusion type equation that contains nonlinear terms that stem from a Landau-Ginzburg-DeGennes potential.

We use a specific model with three viscosity coefficients that allows the contribution of the orientation to the viscous stress to be cast in the form of an orientation-dependent body force. A time-discretised strategy for solving the flow-orientation problem is implemented by using two alternating steps. First, the flow field of the Stokes flow is computed for a given orientation field. This is done using extremely efficient Krylov subspace and multigrid iteration techniques. Then, with the flow field given, one time step of the orientation equation is carried out. The new orientation field is then used to compute a new body force which is again used in the Stokes equation and so forth.

As an example application, we consider lid driven cavity flow. The ensuing non-homogeneous orientation of the Nematic in this geometry leads to non-linear flow effects similar to those known from flow at high Reynolds numbers.

Keywords

Computational Fluid Dynamics, Nematic Liquid Crystals, Alignment Tensor

1 Introduction

The flow of a nematic liquid crystal can be described in various ways. While the most common approach uses the Ericksen-Leslie theory for the nematic director, a more general description using the second rank alignment tensor is needed for problems that involve defects. Different constitutive theories for the alignment tensor have been derived [4, 7, 8, 9], and numerical solutions for some special cases have been produced. The creation of backflow and its influence on the annihilation of defects in two space dimensions has been examined in [14, 15]. In this example, the reorientation of the alignment is the driving force. Also the impact of flow on the orientation has received much attention. Possibly the earliest application was given by Leslie: the flow alignment of the director in a simple shear [6]. The behaviour of the alignment tensor under shear in a monodomain was also extensively studied in [3, 10].

Even in a homogeneous, simple shear flow, many different types of behaviour can be found, such as flow aligning, tumbling, and chaos. Furthermore, to obtain a complete picture, spatially

*Department of Mathematics, University of Strathclyde, Glasgow G1 1XH, Scotland. Tel: +441415483648, Fax: +441415483345, ams@maths.strath.ac.uk

†Department of Mathematics, University of Strathclyde, Glasgow G1 1XH, Scotland. Tel: +441415483801, Fax: +441415483345, ar@maths.strath.ac.uk

inhomogeneous situations have to be considered. The evolution is determined by two equations: the flow is governed by a generalised Navier-Stokes equation, in which the divergence of the stress tensor also depends on the alignment tensor and its time derivative, and the evolution of the orientation is governed by a convection-diffusion type equation that contains nonlinear terms that stem from a Landau-DeGennes potential [12].

In this paper we consider a specific model with three viscosity coefficients that allows us to write the contribution of the orientation to the viscous stress in the form of an orientation dependent body force. We propose a time-discretised strategy for solving the flow-orientation problem that involves two alternating steps. First, for a given flow field, one time step for the orientation equation is carried out according to the methods described in [11]. Then, the flow field of the Stokes flow is computed for the given orientation field. This is done using state-of-the-art Krylov subspace and multigrid iteration techniques [1, 2].

2 Underlying equations

We consider a nematic liquid crystal whose orientational order is described by the second rank alignment tensor $\mathbf{Q}$. If $\boldsymbol{u}$ denotes a unit vector parallel to the symmetry axis of an effectively uniaxial molecule, $\mathbf{Q}$ can be defined as the local average

$$\mathbf{Q} := \langle\, \overline{\boldsymbol{u} \otimes \boldsymbol{u}}\, \rangle = \langle \boldsymbol{u} \otimes \boldsymbol{u} - \frac{1}{3}\mathbf{I} \rangle \tag{1}$$

where $\mathbf{I}$ is the identity tensor and $\overline{\ldots}$ denotes the symmetric traceless part of a tensor.

Equations of motion for flow and alignment can conveniently be formulated in terms of a frame-independent invariant rate of the alignment tensor [13]. We choose the co-rotational time derivative

$$\mathring{\mathbf{Q}} = \dot{\mathbf{Q}} - 2\,\overline{\mathbf{W}\mathbf{Q}} \tag{2}$$

where $\mathbf{W} = \frac{1}{2}(\nabla \boldsymbol{v} - (\nabla \boldsymbol{v})^T)$ is the skew part of the velocity gradient and $\dot{\mathbf{Q}} = \frac{\partial \mathbf{Q}}{\partial t} + (\nabla \mathbf{Q})\boldsymbol{v}$ is the material time derivative of $\mathbf{Q}$. Suppose now that the free energy connected with the alignment is given as a function $W = W(\mathbf{Q}, \nabla \mathbf{Q})$, the dissipation is specified as a function $R = R(\mathring{\mathbf{Q}}, \mathbf{Q}, \mathbf{D})$ that is a quadratic form in $\mathring{\mathbf{Q}}$, and the symmetric part of the velocity gradient is $\mathbf{D} = \frac{1}{2}(\nabla \boldsymbol{v} + (\nabla \boldsymbol{v})^T)$. Then the equations for flow and alignment take the general form [12]

$$\begin{aligned} \rho \dot{\boldsymbol{v}} &= \operatorname{div} \mathbf{T} \\ \frac{\partial W}{\partial \mathbf{Q}} - \operatorname{div} \frac{\partial W}{\partial \nabla \mathbf{Q}} &+ \frac{\partial R}{\partial \mathring{\mathbf{Q}}} = \mathbf{0} \end{aligned} \tag{3}$$

where the stress tensor $\boldsymbol{T}$ is given by

$$\mathbf{T} = -p\,\mathbf{I} - \nabla \mathbf{Q} \odot \frac{\partial W}{\partial \nabla \mathbf{Q}} + \frac{\partial R}{\partial \mathbf{D}} + \mathbf{Q}\,\frac{\partial R}{\partial \mathring{\mathbf{Q}}} - \frac{\partial R}{\partial \mathring{\mathbf{Q}}}\,\mathbf{Q}. \tag{4}$$

This tensor contains an isotropic contribution from the hydrostatic pressure p, a viscous stress with symmetric part $\partial R/\partial \mathbf{D}$ and skew part $\mathbf{Q}\,\partial R/\partial \mathring{\mathbf{Q}} - \partial R/\partial \mathring{\mathbf{Q}}\,\mathbf{Q}$, and an elastic stress

$$\left(\nabla \mathbf{Q} \odot \frac{\partial W}{\partial \nabla \mathbf{Q}}\right)_{ij} := Q_{kl,i} \frac{\partial W}{\partial Q_{kl,j}}$$

which is analogous to the Ericksen elastic stress in a director based description.

To obtain a specific model, we choose the free energy to be of the form

$$W = \phi + \frac{1}{2} L_1 \|\nabla \mathbf{Q}\|^2, \tag{5}$$

where $\phi = \frac{1}{2} A(T) \operatorname{tr} \mathbf{Q}^2 - \frac{\sqrt{6}}{3} B \operatorname{tr} \mathbf{Q}^3 + \frac{1}{4} C (\operatorname{tr} \mathbf{Q}^2)^2$ is a Landau-deGennes potential, and a curvature elastic energy with one elastic constant L_1 is used. For an alignment tensor theory to be consistent with Ericksen-Leslie theory in the case of uniaxial alignment with constant scalar order parameter, the dissipation function R needs to contain at least five terms. The choice

$$R = \frac{1}{2} \zeta_1 \mathring{\mathbf{Q}} \cdot \mathring{\mathbf{Q}} + \zeta_2 \mathbf{D} \cdot \mathring{\mathbf{Q}} + \frac{1}{2} \zeta_3 \mathbf{D} \cdot \mathbf{D} + \frac{1}{2} \zeta_{31} \mathbf{D} \cdot (\mathbf{D}\mathbf{Q}) + \frac{1}{2} \zeta_{32} (\mathbf{D} \cdot \mathbf{Q})^2 \tag{6}$$

with five phenomenological viscosity coefficients ζ_1, ζ_2, ζ_3, ζ_{31}, and ζ_{32} leads to the stress tensor proposed in [9]. Using (5) and (6) in (3) yields the equation for the alignment

$$\zeta_1 \mathring{\mathbf{Q}} = -\mathbf{\Phi} - \zeta_2 \mathbf{D} + L_1 \Delta \mathbf{Q},$$

where $\mathbf{\Phi}$ is the derivative $\partial \phi / \partial \mathbf{Q}$ of the Landau-deGennes potential ϕ. The different contributions to the stress tensor (4) then take the following forms: the skew-symmetric part is

$$\mathbf{T}^{\text{skew}} = \zeta_1 (\mathbf{Q}\mathring{\mathbf{Q}} - \mathring{\mathbf{Q}}\mathbf{Q}) + \zeta_2 (\mathbf{Q}\mathbf{D} - \mathbf{D}\mathbf{Q}) \tag{7}$$

and the symmetric traceless part of the viscous stress is

$$\overline{\mathbf{T}^{(\text{v})}} = \zeta_2 \mathring{\mathbf{Q}} + \zeta_3 \mathbf{D} + \zeta_{31} \overline{\mathbf{D}\mathbf{Q}} + \zeta_{32} (\mathbf{Q} \cdot \mathbf{D})\, \mathbf{Q}. \tag{8}$$

In the one elastic constant approximation, the elastic contribution to the stress is symmetric, and is given by

$$\mathbf{T}^{(\text{e})} = -L_1\, \nabla \mathbf{Q} \odot \nabla \mathbf{Q}. \tag{9}$$

3 Solution Strategy

The first step in solving (3) is to eliminate the time derivative of the alignment tensor from the stress. To this end, we observe that on a solution

$$\mathring{\mathbf{Q}} = \frac{1}{\zeta_1} \left(-\mathbf{\Phi} - \zeta_2 \mathbf{D} + L_1 \Delta \mathbf{Q} \right). \tag{10}$$

Using this in expression (7) for the skew part of the viscous stress, we find that

$$\begin{aligned} \mathbf{T}^{\text{skew}} &= \zeta_1 (\mathbf{Q}\mathring{\mathbf{Q}} - \mathring{\mathbf{Q}}\mathbf{Q}) + \zeta_2 (\mathbf{Q}\mathbf{D} - \mathbf{D}\mathbf{Q}) \\ &= \mathbf{\Phi}\mathbf{Q} - \mathbf{Q}\mathbf{\Phi} + L_1 [\mathbf{Q}(\Delta \mathbf{Q}) - (\Delta \mathbf{Q})\mathbf{Q}] \\ &= L_1 [\mathbf{Q}(\Delta \mathbf{Q}) - (\Delta \mathbf{Q})\mathbf{Q}], \end{aligned} \tag{11}$$

where the last equality holds because $\mathbf{\Phi}$ is a polynomial in $\mathbf{Q}$ that commutes with $\mathbf{Q}$ itself. Applying the same procedure to the symmetric part of the viscous stress yields

$$\overline{\mathbf{T}^{(\text{v})}} = \frac{\zeta_2}{\zeta_1} (L_1 \Delta \mathbf{Q} - \mathbf{\Phi}) + \zeta_4 \mathbf{D} + \zeta_{31} \overline{\mathbf{D}\mathbf{Q}} + \zeta_{32} (\mathbf{Q} \cdot \mathbf{D})\, \mathbf{Q} \tag{12}$$

where we have introduced a renormalised isotropic viscosity ζ_4 according to $\zeta_4 := \zeta_3 - \zeta_2^2 / \zeta_1$.

From now on, we will neglect the last two terms in (12), that is, we will assume that $\zeta_{31} = \zeta_{32} = 0$. In terms of the Leslie viscosities, this amounts to making the assumptions $\alpha_1 = 0$ and $\alpha_5 = -\alpha_6$,

see [12]. We note that while these assumptions are reasonable for small molecule liquid crystals, they will have to be modified for polymeric liquid crystals (see conclusions). The advantage of making these assumptions is that with $\zeta_{31} = \zeta_{32} = 0$, the divergence of the stress tensor takes a very convenient form. In particular, for low Reynolds numbers, when flow inertia can be neglected, setting $\operatorname{div} \mathbf{T} = \boldsymbol{0}$ leads to

$$\begin{gathered} \nabla p - \tfrac{1}{2}\zeta_4 \Delta \boldsymbol{v} = \operatorname{div} \mathbf{F} \quad \text{with} \\ \mathbf{F} = L_1 \Big(\mathbf{Q}(\Delta \mathbf{Q}) - (\Delta \mathbf{Q})\mathbf{Q} + \tfrac{\zeta_2}{\zeta_1} \Delta \mathbf{Q} - \nabla \mathbf{Q} \odot \nabla \mathbf{Q} \Big) - \tfrac{\zeta_2}{\zeta_1} \mathbf{\Phi}. \end{gathered} \tag{13}$$

We non-dimensionalise equations (10) and (13) by expressing all lengths in terms of the nematic coherence length $\xi = \sqrt{9CL_1/(2B^2)}$ and all times in terms of the relaxation time $\tau_1 = 9C\zeta_1/(2B^2)$. In addition, we rescale the alignment tensor according to $\tilde{\mathbf{Q}} = 3C/(2B)\,\mathbf{Q}$. This leads to the dimensionless Landau-deGennes potential

$$\tilde{\mathbf{\Phi}} = (\vartheta + 2 \operatorname{tr} \tilde{\mathbf{Q}}^2)\tilde{\mathbf{Q}} + 3\sqrt{6}\, \overline{\tilde{\mathbf{Q}}\tilde{\mathbf{Q}}}, \tag{14}$$

where $\vartheta = 9C/(2B^2)\, A(T)$ is a dimensionless temperature parameter. In these units, the clearing point T_c and the pseudo critical temperature T^* correspond to $\vartheta = 1$ and $\vartheta = 0$, respectively [5]. Note that, for convenience, the tildes are dropped in all subsequent formulae. The dimensionless equations then are

$$\mathring{\mathbf{Q}} = \Delta \mathbf{Q} - \mathbf{\Phi} - \mathrm{Tu}\, \mathbf{D}$$

for the orientation and

$$\begin{gathered} \nabla p - \Delta \boldsymbol{v} = \operatorname{div} \mathbf{F}, \\ \mathbf{F} = \mathrm{Bf} \left\{ \tfrac{1}{\mathrm{Tu}} \left[\mathbf{Q}(\Delta \mathbf{Q}) - (\Delta \mathbf{Q})\mathbf{Q} - \nabla \mathbf{Q} \odot \nabla \mathbf{Q} \right] + \Delta \mathbf{Q} - \mathbf{\Phi} \right\} \end{gathered} \tag{15}$$

for the flow, where we have introduced two more dimensionless parameters: one, the *backflow parameter* $\mathrm{Bf} = 4B\zeta_2/(3C\zeta_4)$, measures the impact of the orientation on the flow, and the other, the *tumbling parameter* $\mathrm{Tu} = 3C\zeta_2/(2B\zeta_1)$, measures the relative strength of the viscosities ζ_2 and ζ_1. For a uniaxial state with equilibrium order at $T = T_c$ we have $\mathrm{Tu} = \gamma_2/\gamma_1$. In a simple shear one can expect flow alignment for $\mathrm{Tu} > 1$, where the liquid crystal aligns at an angle of $\cos 2\phi_a = -1/\mathrm{Tu}$ to the direction of the flow gradient [6]. For values of $\mathrm{Tu} < 1$ some dynamic state such as tumbling should prevail.

Equation (15) is simply a Stokes equation with a body force that is the divergence of a tensor $\mathbf{F}$ that depends only on $\mathbf{Q}$ and its spatial derivatives. This suggests the following iterative strategy for the solution of the coupled flow-orientation problem:

1. For a given orientation field $\mathbf{Q}$, solve the Stokes equation with $\operatorname{div} \mathbf{F}$ as a body force using standard methods of computational fluid dynamics.

2. Use the obtained flow field to compute one time step in a discretised version of the orientation equation.

3. With the new orientation field, go back to step 1.

This strategy was implemented using a finite difference discretisation of the orientation equation with explicit time stepping. The Stokes equation was solved at each step using a finite element iterative solver adapted from the public domain MATLAB package IFISS [1]. Specifically, the Stokes solver used a Taylor-Hood mixed finite element approximation with the resulting linear system being solved via a preconditioned MINRES solver. The block diagonal preconditioner used (which involved applying one V-cycle of geometric multigrid to the Laplacian component and scaling the Schur complement part with the diagonal of the pressure mass matrix) is known to be very efficient and effective for Stokes problems [2].

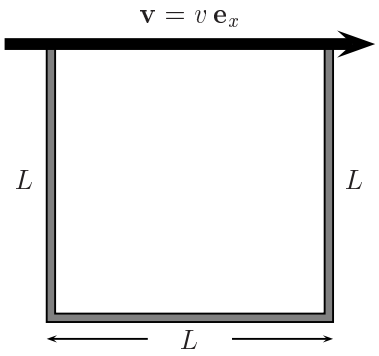

Figure 1: Specification of lid driven cavity problem.

4 Flow in a Lid Driven Cavity

The lid driven cavity is a classic test problem in fluid dynamics where flow in a square cavity is driven by the lid moving from left to right, see Figure 1. The flow boundary conditions are of Dirichlet type everywhere, with the velocity fixed at some positive rate in the x-direction on the lid and zero along all other cavity walls. Here we use a 'watertight' cavity, that is, the velocity is fixed to be zero at the top corner points on both left and right boundaries. The resulting discontinuous horizontal velocity generates a strong singularity in the pressure solution, but away from these corners the pressure is essentially constant.

Dirichlet boundary conditions are also used for the alignment tensor. The same uniaxial alignment with equilibrium order parameter is prescribed at all boundaries and also as an initial condition in the bulk. In this way, without driving flow a homogeneous uniaxial orientation would result.

4.1 In-Plane Orientation

For a pure in-plane evolution, we used homeotropic anchoring on the top and bottom of the cavity and planar anchoring on the lateral sides. The initial orientation and results with $v = 10$ and $L = 8$ are shown in Figure 2. This corresponds to a Reynolds number of $\mathrm{Re} = VL\rho/\zeta_4 \approx 10^{-5}$ for a typical small-molecule liquid crystal. The Ericksen number is then $\mathrm{Er} = \zeta_1 VL/L_1 \approx 80$, and we chose $\mathrm{Bf} = 2/3$ and $\mathrm{Tu} = 1/5$. The temperature was chosen as $\vartheta = 0$, corresponding to the pseudo-critical temperature T^*. The boxes shown lie parallel to the eigensystem of the alignment tensor, and the lengths of the edges correspond to the respective eigenvalues, see [11]. The shading of the box shows its degree of biaxiality: a white box corresponds to uniaxial alignment, and the degree of colour in the other boxes is proportional to the biaxiality measure $\beta^2 = 1 - 6(\mathrm{tr}\,\mathbf{Q}^3)^2/(\mathrm{tr}\,\mathbf{Q}^2)^3$ used in [5].

The evolution displayed in the right picture in Figure 2 shows two distinct types of orientation. On the one hand, in the lower part of the cavity, the orientation is dominated by the elastic forces and a stationary state of aligned flow is found. On the other hand, close to the lid where the velocity gradient is large, a periodic solution of in-plane tumbling orientation is found. Furthermore, because of the fixed boundary conditions, the orientation necessarily shows defects. In the alignment tensor description, these defects are characterised by a planar uniaxial orientation. They are generated close to the upper right corner of the lid and travel towards the centre of the cavity and from there to the upper left corner.

For the given choice of the parameters, the flow field is only slightly affected by the orientation (see Figure 3). Initially, with a homogeneous orientation, the stream lines are symmetric about a vertical axis through the centre of the cavity. This reflects the time-reversal symmetry of the

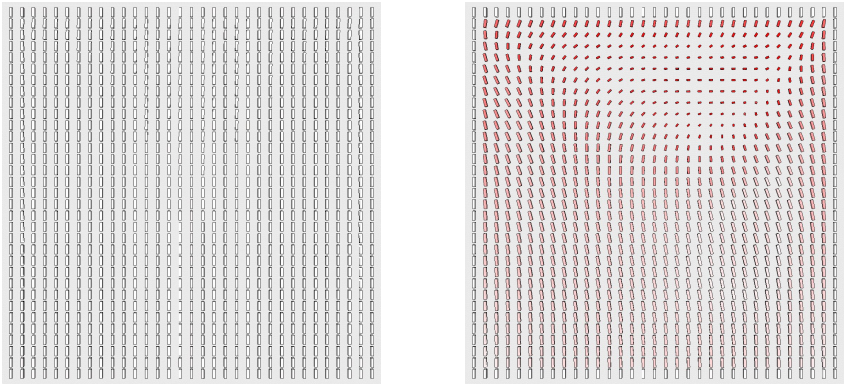

Figure 2: *In-plane orientation.* The initial homogenous orientation with fixed boundary conditions is shown on the left. The non-homogeneous alignment field caused by the moving lid (on the right) shows regions of flow alignment in the lower part of the cavity and a periodic tumbling alignment close to the lid. There, the scalar order parameter is reduced significantly, as is visible from the smaller size of the boxes.

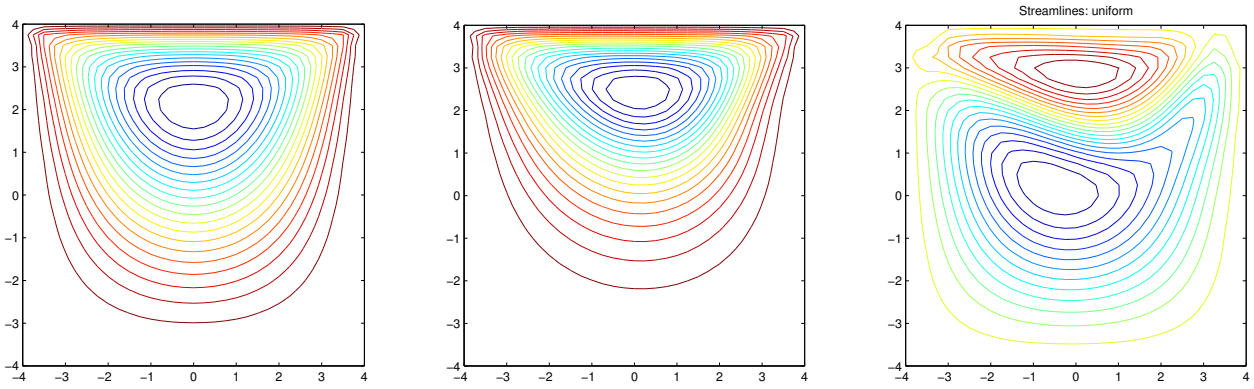

Figure 3: *Flow field during the evolution.* The left picture shows the streamlines of the flow field for the initial homogenous configuration: they are symmetric with respect to a vertical axis through the centre of the cavity. The picture in the middle shows the streamlines at later time, which are no longer symmetric but, due to the changes in the orientation field, are shifted slightly to the right. The rightmost picture shows a contour plot of the difference between the two flow fields.

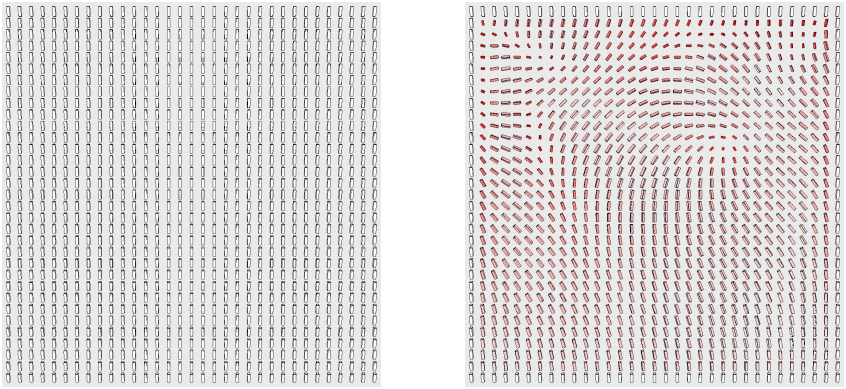

Figure 4: *Out-of-plane orientation.* The initial orientation (on the left) is again homogenous; with respect to the in-plane orientation, the top of the alignment tensor is tilted by 15° out of the plane towards the observer. On the right, in the lower part of the cavity, the orientation is again one of flow alignment, which is out of the plane. Close to the lid, a periodic kayaking solution is found and, as in the in-plane case, defects are created in the upper right corner and eventually annihilate in the upper left corner. The reduction of order is considerably less pronounced than in the in-plane case.

Stokes equation. When the orientation is no longer homogenous, this symmetry is broken and the streamlines shift to the right. This is an effect similar to that found in isotropic fluids at high Reynolds numbers. It is found here in a linear flow equation because of the influence of the orientation on the flow.

4.2 Out-of-Plane Orientation

To obtain an out-of-plane evolution, both the boundary and initial conditions were tilted by an angle of 15° out of the shear plane. Here we used $v = 15$ and $L = 16$, which corresponds to a Reynolds number of 3×10^{-5} and an Ericksen number of 240. As before, $\mathrm{Bf} = 2/3$ and $\vartheta = 0$, but here we chose $\mathrm{Tu} = 4/5$ to facilitate the occurence of out-of-plane periodic solutions (see, for example, the phase diagrams for monodomains in [3]).

The resulting evolution (as shown in Figure 4) again shows in the lower part of the cavity a region of flow alignment that here is out of the plane. Close to the lid, periodic kayaking is found, again accompanied by the creation of defects in the upper right corner and their annihilation in the upper left corner. A notable difference from the in-plane evolution is that the reduction of the scalar order parameter is far less pronounced. Here, it takes place mostly around the defects: the orientation can go out of the plane to avoid the frustration induced by the flow gradient.

When the orientation has components that lie out of the plane, the body force $\operatorname{div}\mathbf{F}$ that is generated by the viscous stress can have a component that lies out of the plane even when both flow field and orientation field are assumed to be homogeneous in that direction. This out-of-plane component of $\operatorname{div}\mathbf{F}$ is shown in Figure 5. It is most noticeable at the corners where the pressure is divergent, but it is present throughout the cavity. This shows that, for out-of-plane evolutions, truly three-dimensional flow fields will arise and that two-dimensional computations are therefore only of limited value.

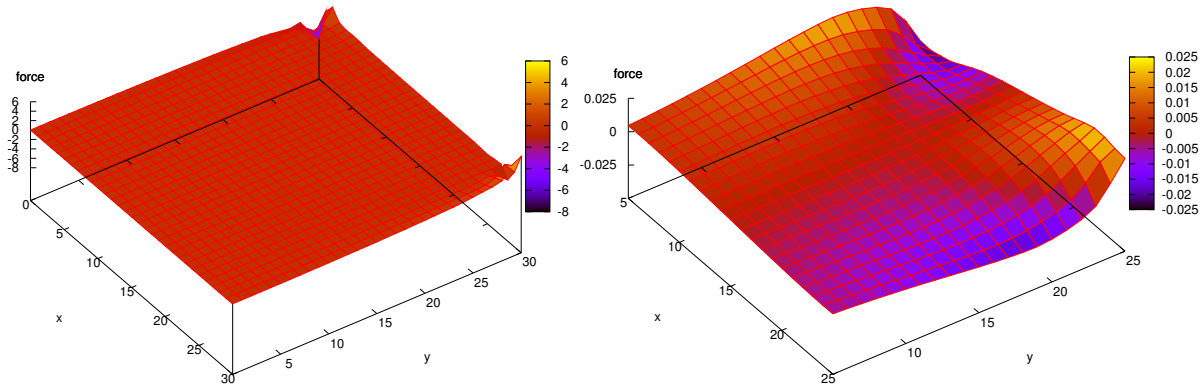

Figure 5: *Component of the body force perpendicular to the shear plane.* This force component is particularly large at the corners where the pressure is divergent (left) but it is present throughout the cavity, as evidenced by the close-up of the central region (right).

5 Conclusions

In this paper, we have described a highly efficient algorithm for the computation of flow and orientation in nematic liquid crystals. Writing the influence of the orientation field on the flow in the form of a body force allows us to solve the flow equation by using well established fast solvers. This aspect of the modelling dominates the computational time required, so that the overhead added to the computational fluid dynamics by the anisotropic liquid is rather small.

One disadvantage of the method that we have presented is that only three viscosity coefficients enter the viscous stress. However, when the co-rotational time derivative that we have used here is replaced by a general co-deformational time derivative

$$\mathring{\mathbf{Q}} = \dot{\mathbf{Q}} - 2\,\overline{\mathbf{WQ}} - 2\sigma\,\overline{\mathbf{DQ}}\,,$$

the same numerical procedure as before can be employed. As long as only the terms proportional to ζ_1, ζ_2, and ζ_3 are considered in the dissipation function, the influence of the orientation on the flow still takes the form of a body force (although comparison with Ericksen-Leslie theory shows that all five viscosities for uniaxial alignment are different from zero in this case [12, 8]). This makes the type of algorithm presented in this paper suitable for a more general class of materials, such as polymeric liquid crystals.

Generalisation to high Reynolds numbers is also straightforward: it requires the retention of the inertial term $\rho\dot{\boldsymbol{v}}$ on the left hand side of (15) and solution of the resulting Navier-Stokes equation with a specified body force. The latter could be efficiently achieved using the advanced preconditioned iterative techniques for finite element Navier-Stokes approximations described in [2].

Acknowledgements

AR acknowledges support for this work from EPSRC through grant EP/C53154X/1. AMS acknowledges support from The Leverhulme Trust through a Research Fellowship.

References

[1] Elman HC, Ramage A, Silvester DJ (2007) Algorithm 886: IFISS, Incompressible Flow & Iterative Solver Software, ACM T. Math. Software 33

[2] Elman HC, Silvester DJ, Wathen AJ (2005) Finite Elements and Fast Iterative Solvers with applications in incompressible fluid dynamics, Oxford, UK: Oxford University Press

[3] Grosso M, Maffettone PL, Dupret F (2000) A closure approximation for nematic liquid crystals based on the canonical distribution subspace theory, Rheol. Acta 39: 301–310

[4] Hess S (1975) Irreversible thermodynamics of nonequilibrium alignment phenomena in molecular liquids and in liquid crystals, Z. Naturforsch. 30a: 728–738 & 1224–1232

[5] Kaiser P, Wiese W, Hess S (1992) Stability and instability of an uniaxial alignment against biaxial distortions in the isotropic and nematic phases of liquid crystals, J. Non-Equilib. Thermodyn. 17: 153–169

[6] Leslie FM (1968) Some constitutive equations for liquid crystals, Arch. Rational Mech. Anal. 28: 265–283

[7] Olmsted PD, Goldbart P (1990) Theory of the nonequilibrium phase transition for nematic liquid crystals under shear flow, Phys. Rev. A 41: 4578–4581

[8] Pereira Borgmeyer C, Hess S (1995) Unified description of the flow alignment and viscosity in the isotropic and nematic phases of liquid crystals, J. Non-Equilib. Thermodyn. 20: 359–384

[9] Qian T, Sheng P (1998) Generalized hydrodynamic equations for nematic liquid crystals, Phys. Rev. E 58: 7475–7485

[10] Rienäcker G, Hess S (1999) Orientational dynamics of nematic liquid crystals under shear flow, Physica A 267: 294–321

[11] Sonnet A, Kilian A, Hess S (1995) Alignment tensor versus director: Description of defects in nematic liquid crystals, Phys. Rev. E 52: 718–722

[12] Sonnet AM, Maffettone PL, Virga EG (2004) Continuum theory for nematic liquid crystals with tensorial order, J. Non-Newtonian Fluid Mech. 119: 51–59

[13] Sonnet AM, Virga EG (2001) Dynamics of dissipative ordered fluids, Phys. Rev. E 64: 031705

[14] Svenšek D, Žumer S (2002) Hydrodynamics of pair-annihilating disclination lines in nematic liquid crystals, Phys. Rev. E 66: 021712

[15] Tóth G, Denniston C, Yeomans JM (2002) Hydrodynamics of topological defects in nematic liquid crystals, Phys. Rev. Lett. 88: 105504